# Exploratory Study of Interplanetary Trajectories for a Twin-Spacecraft Mission to the Ice Giants

Georgia Tech Space Systems Design Laboratory
School of Aerospace Engineering

AE 8900 MS Special Problems Report

Space Systems Design Lab (SSDL)
Daniel Guggenheim School of Aerospace Engineering
Georgia Institute of Technology, Atlanta, GA

Author:
Bhavi Jagatia

Advisor:
Dr. Brian C. Gunter

May 14, 2021

# EXPLORATORY STUDY OF INTERPLANETARY TRAJECTORIES FOR A TWIN-SPACECRAFT MISSION TO THE ICE GIANTS

**Bhavi Jagatia**
Georgia Institute of Technology
bhavi.jagatia@gatech.edu

Uranus, and Neptune, the Ice Giants, can provide unique insights into the formation of the solar system, and answer pressing planetary science questions. A combined mission to both ice giants would provide double the science return than visiting an individual ice giant. This work aims to investigate feasible trajectories for such a twin-spacecraft single-launch mission to the ice giants. The analysis considers chemically propelled trajectories and solves the Powered Multiple Gravity Assist global optimization problem. Recommendations are made for feasible trajectories based on $\Delta\mathbf{v}$, mission duration, and science return.

## INTRODUCTION

Exploring Uranus and Neptune—the icy giants— is imperative to completing our understanding of the solar system and beyond (exoplanets). The closest observations of the ice giants were obtained during the Voyager 2 fly-bys of the two planets in 1986/9. Since then, most solar system exploration missions have been focused on reachable planets, namely the inner planets and gas giants. Missions to the ice giants have longer flight times, expensive $\Delta\mathbf{v}$, and reduced payload masses.

Uranus and Neptune exploration offers unique insight into the creation of the solar system. While the gas giants are known to be composed of hydrogen and helium in both the metallic and gaseous forms, and the terrestrial planets are primarily composed of silicate rock and metal, the ice giants are largely believed to be composed of supercritical water and methane. In addition to compositional differences, the ice giants' systems present unexplored phenomena—complex off-center magnetic fields, radiation belts, and unique rings and satellites. Moreover, understanding the composition of ice giants could provide invaluable insight into understanding exoplanets; most discovered exoplanets have similar masses as the ice giants. Current solar system models cannot account for the formation of the ice giants without requiring significant deviations; expanding these models based on findings from the icy giants would help immensely with understanding the formation of exoplanets.

The 2013-22 planetary decadal survey proposed a mission to Uranus as its 3rd priority, after Mars Perseverance and Europa Clipper. Given the progress of these two missions, the next decade will ideally focus on missions to the ice giants. In this vein, JPL conducted a pre-decadal survey, curating the desired science return, and creating and evaluating architectures that could provide those. These architectures consisted of either Uranus or Neptune missions with a combination of fly-bys, orbiters, and probes. One standout architecture, that ranked highest for science return, was a single launch, twin-spacecraft mission to both Uranus and Neptune. This would allow for a comparative study of the ice giants and be cheaper to develop because the payloads to each planet would ideally look the same. If only a single ice giant mission architecture was picked, then there would inevitably have to be a second one to the other ice giant in the future. Therefore, the twin-spacecraft mission provides an opportunity for maximal science return in a single flagship class mission and holds scope to complete our solar system exploration within a single mission.

Given the preliminary nature of the JPL study, they chose to explore the more established mission architectures in detail. These included single planet missions to either Uranus or Neptune.

The twin spacecraft mission architecture was proposed but not studied further. This study is motivated by the potential of a twin-spacecraft mission and aims to find feasible trajectories for both Ice Giant exploration in the 2025-2050 period. The long launch period was chosen to allow for missions that could study the equinoxes in 2040/46 at Uranus and Neptune, respectively.

The analysis defines a global optimization problem for powered multiple gravity assist (PMGA) trajectories, with the objective of minimization of fuel consumption. This optimization problem is modified to incorporate variations of flyby scenarios, arrival conditions, and launch windows. The problem is solved to generate a set of 250,000 candidate trajectories. Once evaluated, the optimal trajectories are compared to find those with the most science return and feasibility. Recommendations are made for scenarios to explore further.

The analysis is conducted using the open-source Python and C++ libraries PyKEP and PyGMO. PyKEP provides computational astrodynamics tools and PyGMO provides algorithms for implementing large-scale global optimization problems.

## METHODOLOGY

Preliminary interplanetary trajectory design is usually conducted using the patched conics approximation; wherein each body that the spacecraft interacts with has its own calculated sphere of influence (SOI) and within that SOI, only the gravitational influence that body is considered.

Upon adding a few simplifications, this problem can be expressed as an optimization problem with the objective being minimization of time of flight or total $\mathbf{\Delta v}$ (and therefore, propellant used). This section will discuss: (1) modeling interplanetary trajectories with a patched conic approximation, (2) defining the optimization problem for multiple gravity assist trajectories, and (3) refining the optimization problem for the twin-spacecraft mission.

### Trajectory Model

Per the patched conic approximation, interplanetary trajectories are modeled in segments: (1) travel within planetary SOI (launch and fly-bys), (2) interplanetary transfer legs, (3) capture at target planet.

Travel within the SOI is modeled as a two-body problem, with the assumption that the only gravitational forces on the spacecraft are due to the planet. Outside of the SOI, it is assumed that the spacecraft is only gravitationally interacting with the sun. At the border of the SOI, when the spacecraft is exiting, the spacecraft's exit velocity (with reference to the planet), also called the spacecraft *hyperbolic excess velocity*, is added to the planet's heliocentric velocity. The resulting velocity is the spacecraft's heliocentric velocity during the interplanetary transfer at that point in the journey. In this analysis, for vector representation, the subscripts $\mathbf{v}_{ab}$ represent a vector of $b$ with respect to $a$. In Equation (1), the subscripts s represents sun, v represents vehicle/spacecraft, and p represents planet.

$$\mathbf{v}_{sv} = \mathbf{v}_{sp} + \mathbf{v}_{vp} \tag{1}$$

During the interplanetary transfer leg, the spacecraft is influenced only by sun's gravity. Thus, given the initial $\mathbf{v}$ at the prior planetary encounter, the spacecraft motion can be propagated ahead and the velocity at the next planetary encounter can be determined.

*Planetary fly-by*. Planetary fly-by maneuvers are often employed in interplanetary missions as a means of modifying the spacecraft velocity without expending fuel. By utilizing the gravity field of the planet, the spacecraft's hyperbolic excess velocity can be modified in speed and direction.

Figure 1 shows the velocity vector diagram for a flyby. $\mathbf{v}_{in}$ and $\mathbf{v}_{out}$ represent the spacecraft velocity vectors before and after the fly-by. Since the spacecraft is within the planet's SOI and is only acted upon by the planet's gravity, its energy relative to the planet is conserved during the flyby hyperbola. Thus, the velocities $\mathbf{v}_{\infty,in}$ and $\mathbf{v}_{\infty,out}$ are equal in magnitude. Despite $\mathbf{v}_{\infty,in}$ and $\mathbf{v}_{\infty,out}$ being equal in magnitude, the directional change caused during the flyby provides a $\Delta\mathbf{v}$ to the spacecraft heliocentric velocity (observed by the vector difference in $\mathbf{v}_{sv,in}$ and $\mathbf{v}_{sv,out}$).

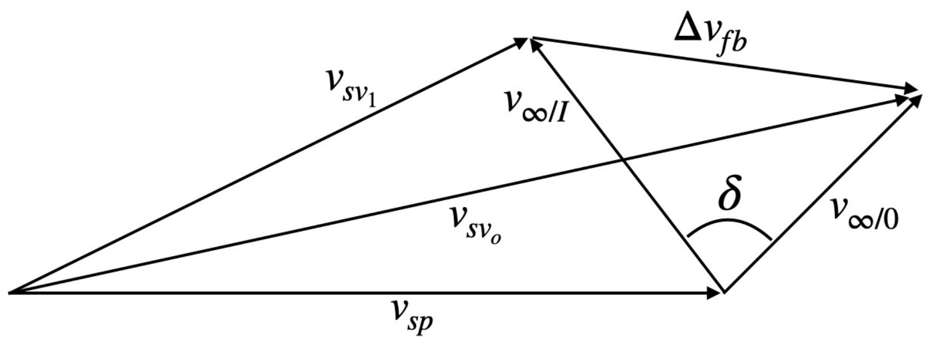


**Figure 1. Velocity vector diagram for a planetary flyby.**

The value of the spacecraft velocity after flyby, $\mathbf{v}_{sv,out}$, can be determined using the following equation

$$\begin{gathered}\Delta\mathbf{v}_{flyby} = \mathbf{v}_{sv,out} - \mathbf{v}_{sv,in} = \mathbf{v}_{\infty,out} - \mathbf{v}_{\infty,in} \\ \mathbf{v}_{sv,out} = \mathbf{v}_{sv,in} + \mathbf{v}_{\infty,out} - \mathbf{v}_{\infty,in}\end{gathered} \tag{2}$$

For the optimization analysis, it is useful to obtain $\Delta\mathbf{v}_{flyby}$ as a function of the spacecraft hyperbolic excess velocity, radius of periapsis, and the planet's parameters (heliocentric velocity, radius),

$$\begin{gathered}\Delta\mathbf{v}_{flyby} = 2\mathbf{v}_{\infty} sin\frac{\delta}{2} \\ \frac{\Delta\mathbf{v}_{flyby}}{\mathbf{v}_s} = \frac{\frac{2\mathbf{v}_{\infty}}{\mathbf{v}_s}}{1+\left(\frac{\mathbf{v}_{\infty}}{\mathbf{v}_s}\right)^2\left(\frac{r_p}{r_s}\right)}\end{gathered} \tag{3}$$

While gravity-assist flybys can provide significant heliocentric $\Delta\mathbf{v}$s, powered flybys are an efficient way to gain additional energy. Also known as Oberth maneuvers, powered flybys are maneuvers wherein a spacecraft applies an impulse during the incoming flyby hyperbola, to provide a greater gain in kinetic energy than can be achieved by applying a similar impulse outside of the flyby. This maneuver is especially useful for modeling the trajectory for optimization problems; the maneuver allows accounting for changes in the spacecraft hyperbolic excess velocity magnitude before and after a flyby. In the patched conics assumption, a powered flyby provides an instantaneous transfer between two consecutive transfer legs with differing boundary velocities.

For the scope of this model, it is assumed that the spacecraft provides instantaneous thrust. To maximize efficiency, the thrust is applied when the spacecraft is at its closest approach to the flyby planet. The $\mathbf{\Delta v}$ required for this maneuver is given by,

$$\mathbf{\Delta v} = \left| \sqrt{\frac{1}{a_i^{in}} + \frac{2}{r_p}} - \sqrt{\frac{1}{a_i^{out}} + \frac{2}{r_p}} \right| \tag{4}$$

where $a_i^{in}$, $a_i^{out}$ represent the semi-major axis of the incoming and outgoing hyperbola respectively, and $r_p$ represents the radius of the planet.

*Capture*. Upon arrival at the destination planet, the spacecraft can either perform a flyby or be captured into a target orbit. For this analysis, it is assumed that slowing down to be captured into an orbit will be performed by an impulsive burn at the capture orbit's periapsis. To explore different methods of capture, such as aerobraking, the analysis will also be performed without any target orbit capture requirements. In this case, the arrival $\mathbf{\Delta v}$ will be the the difference between the heliocentric spacecraft velocity and the heliocentric planet velocity at the planet's SOI boundary,

$$\mathbf{\Delta v}_{arrival} = |\mathbf{v}_{sp} - \mathbf{v}_{sv}| \tag{5}$$

To be captured into an orbit, additional $\mathbf{\Delta v}$ must be applied to slow the spacecraft to the planet's heliocentric velocity,

$$\mathbf{\Delta v}_{capture} = |\mathbf{v}_{sp} - \mathbf{v}_{p,orbit}| \tag{6}$$

where $\mathbf{v}_{p,orbit}$ is calculated at the periapsis of the capture orbit, so as to maximize the orbital velocity, and thus, minimize the $\mathbf{\Delta v}$. This $\mathbf{\Delta v}$ can be expressed in terms of capture orbit parameters—radius of periapsis, $r_p$, and eccentricity, $e$,

$$\mathbf{\Delta v}_{capture} = v_\infty \left( \sqrt{\frac{2\mu}{r_p v_\infty^2} + 1} - \sqrt{\frac{\mu(1+e)}{r_p v_\infty^2}} \right) \tag{7}$$

**Optimization Formulation**

To find trajectories with that satisfy the conditions described above, while utilizing the least amount of fuel, a powered multiple gravity assist (PMGA) optimization problem is defined.

The decision vector is defined as $\mathbf{x} = [T_d, T_1, T_2, \ldots, T_{n+1}]$ where $n$ represents the number of planets to be used for flyby maneuvers. Thus, the spacecraft interacts with $n$+2 planets, including launching from earth and arrival at Uranus/Neptune. The elements of the decision vector are the departure epoch ($T_d$), followed by times of flight for each interplanetary leg.

The goal of the optimization problem is to find a decision vector x such that the total fuel consumed is minimized, and therefore, total payload mass is maximized:

*find*: Decision vector **x**

*with objective*: minimize $\Delta\mathbf{v}$

*with constraints*: launch C3, times of flight, binary for capture at arrival

The process for evaluation, explained later in detail, is:

- Choose random decision vector **x**
- Solve $n$+1 Lambert problems
- Compute all combinations of trajectories
- Find total $\Delta\mathbf{v}$ for each combination

For any decision vector **x**, the corresponding trajectory is computed by identifying a series of interplanetary transfer trajectories. These individual trajectories are calculated by solving Lambert's problem. Each interplanetary transfer leg is a solution of the following boundary value problem:

$$t_2 - t_1 = f(a, c, r_1 + r_2) \tag{8}$$

Where $t_1, t_2$ represent the instant at which the spacecraft is at planet 1 and 2 respectively, $t_2 - t_1$ represents the time of flight, and $a$ and $c$ represent the conic section parameters of the transfer orbit. However, since the transfer orbit is yet to be determined, Equation 8 is not yet in a closed form. Upon further analysis, it can also be expressed as follows:

$$\sqrt{\mu}(t_2 - t_1) = a^{3/2}[\alpha - \beta - (\sin\alpha - \sin\beta)] \tag{9}$$

Where,

$$\sin\left[\frac{\alpha}{2}\right] = \sqrt{\left[\frac{s}{2a}\right]} \tag{10}$$

$$\sin\left[\frac{\beta}{2}\right] = \sqrt{\left[\frac{s-c}{2a}\right]} \tag{11}$$

$$s = \frac{r_1 + r_2 + c}{2} \tag{12}$$

The solution set for a Lambert problem is usually of size 2, ie, the trajectory can either follow the short-duration arc or the long duration arc. However, the problem also admits solutions for that are more than a complete revolution, ie, $\theta > 2\pi$. These solutions, called multiple-revolution solutions, are non-unique. Allowing for multi-revolution solutions gives a total of $2(1 + 2N)$ solutions, where $N$ belongs to $[0,\infty]$. The complete trajectory is formed of $n$+1 interplanetary transfer legs, with each branch being a solution to a multi-revolution Lambert problem. Thus, the total number of candidate trajectories, per decision vector, is given by are product summation from 0 to n $2(1 + 2N)$.

For each candidate trajectory, the values of $\Delta\mathbf{v}$ are computed at every node to evaluate the objective function. First, the launch $\Delta\mathbf{v}$ is computed at epoch $T_d$ using the difference of the spacecraft and Earth heliocentric velocities,

$$\Delta\mathbf{v}_0 = |\mathbf{v}_{sp} - \mathbf{v}_{sv}| \tag{13}$$

Then, the $\Delta\mathbf{v}$ from the difference in velocities at the consecutive interplanetary transfer legs is to be evaluated. Solving the Lambert problem provides the heliocentric velocities of the spacecraft at the beginning ($\mathbf{v}_{i,beg}$) and end ($\mathbf{v}_{i,end}$) of each transfer leg, where the subscript $i$ represents the respective transfer leg. However, for two consecutive legs, $\mathbf{v}_{i,end}$ of the first leg may not equal $\mathbf{v}_{i+1,beg}$ of the second leg. This occurs in case of powered flybys, or Oberth maneuvers as discussed above. In that case, the impulsive $\Delta\mathbf{v}$ to be applied at the periapsis of the flyby maneuver is calculated. Additionally, the spacecraft is required to provide a velocity change to slow down in order to rendezvous with the destination planet. This change in velocity is calculated as the difference in heliocentric velocity of the spacecraft and the destination planet,

$$\Delta\mathbf{v}_{n+1} = |\mathbf{v}_{sp} - \mathbf{v}_{sv}| \tag{14}$$

This method is used to calculate the total $\Delta\mathbf{v}$ for all trajectories. Of these, the trajectory with the minimum $\Delta\mathbf{v}$ is selected.

```
Algorithm 1: PMGA Optimization
Result: Optimal trajectory states at each epoch
randomly generate decision vector;
epochs = decision vector;
for length (decision vector) do
  | compute states at epochs;
end
for length (decision vector) do
  | solve Lambert problem for each leg;
end
for length (decision vector) - 1 do
  | compute powered flyby delta-v;
end
compute capture delta-v;
compute total delta-v;
compare solution with prior solution;
reevaluate decision vector;
```

**Figure 2. Algorithm for implementation of powered multiple gravity assist (PMGA) trajectory optimization problem. The decision vector is generated and evaluated using a global optimization algorithm.**

**Problem Definition**

*Parameters*. The trajectories modeled for the twin-spacecraft, twin-planet mission are based on the following assumptions:

- Spacecraft propulsion:

The spacecraft are assumed to be propelled by mono- or bi-propellant chemical propellant systems that support deep-space maneuvers. Chemical propellant systems allow for the impulsive high-thrust modeled for the powered fly-by maneuvers. Using a bi-propellant system allows for the high $\Delta\mathbf{v}$ maneuvers required for orbit insertion at Uranus and Neptune.

The trajectory model can be modified to include solar electric propulsion and nuclear electric propulsion technologies. These propellant options provide reduced fuel mass, thus allowing for an increase in mass delivered to the destinations.

- Launch velocity:

Instead of considering specific launch vehicles for the analysis, the hyperbolic excess velocity, $\mathbf{v}_\infty$, for Earth launch was specified. A maximum C3 of 170 $km^2/s^2$ was considered; this is equivalent to the launch C3 for New Horizons, the highest currently. This equates to a hyperbolic excess velocity of 13 $km/s$. The optimizer uses the maximum $\mathbf{v}_\infty$ as an upper bound constraint and finds the optimal $\mathbf{v}_\infty$ required for each trajectory. Thus, the analysis thus leaves room for choosing any launch vehicle that is capable of providing the required launch C3; however, the primary candidates are the Atlas V, Delta IV Heavy, SLS, and Starship.

- Orbit insertion:

The trajectories are designed such that upon arrival at Uranus and Neptune, the spacecraft is captured into an elliptical orbit around the destination planet. However, this maneuver is made difficult due to the lack of knowledge about the planets' atmosphere and rings, and the high arrival velocities.

Since the planets are significantly distant from the Sun (Uranus ~20 AU, Neptune ~30 AU ), the spacecraft arrival velocities are high for trajectories with acceptable time of flight. These high arrival velocities lead to high capture $\Delta\mathbf{v}$. Attempts are made to minimize the $\Delta\mathbf{v}$ by designing the capture orbit to be highly eccentric (e = 0.95) and reducing the periapsis radius to a minimum.

Additionally, both Neptune and Uranus have rings and it is vital for the spacecraft to not cross through the rings. In the pre-decadal study survey, the science investigation team's recommendations for a safe orbit insertion radius was $\approx 1.05R_{planet}$ or $\geq 1.05R_{planet}$. Since minimizing the periapsis radius is crucial to minimizing $\Delta\mathbf{v}$, a periapsis of $1.05R_{planet}$ is chosen; this ensures that the spacecraft passes between the innermost ring and the planet to avoid collisions during plane-crossing. A closer periapsis also allows for higher quality data of the planets' gravity and magnetic fields.

Despite the techniques implemented to slow the arrival of the spacecraft at the ice giants, the arrival velocities may still be too high for the spacecraft to insert into an orbit around the planets if solely a bi-propellant chemical system is used. For arrival velocities in the range of 5 km/s to 9.5 km/s, alternative orbit insertion techniques can be implemented, such as aerocapture and radio electric propulsion (REP). Aerocapture is the technique of using atmospheric drag to reduce the velocity of a spacecraft so as to capture it in orbit. While there are additional concerns regarding heat rates and g-loads, aero capture does provide a viable solution for an ice giant orbit insertion. In contrast, an REP engine provides high specific impulse and can be useful to provide large velocity changes at arrival. However, it is constrained by the mass of the REP propulsion system relative to the mass of the payload.

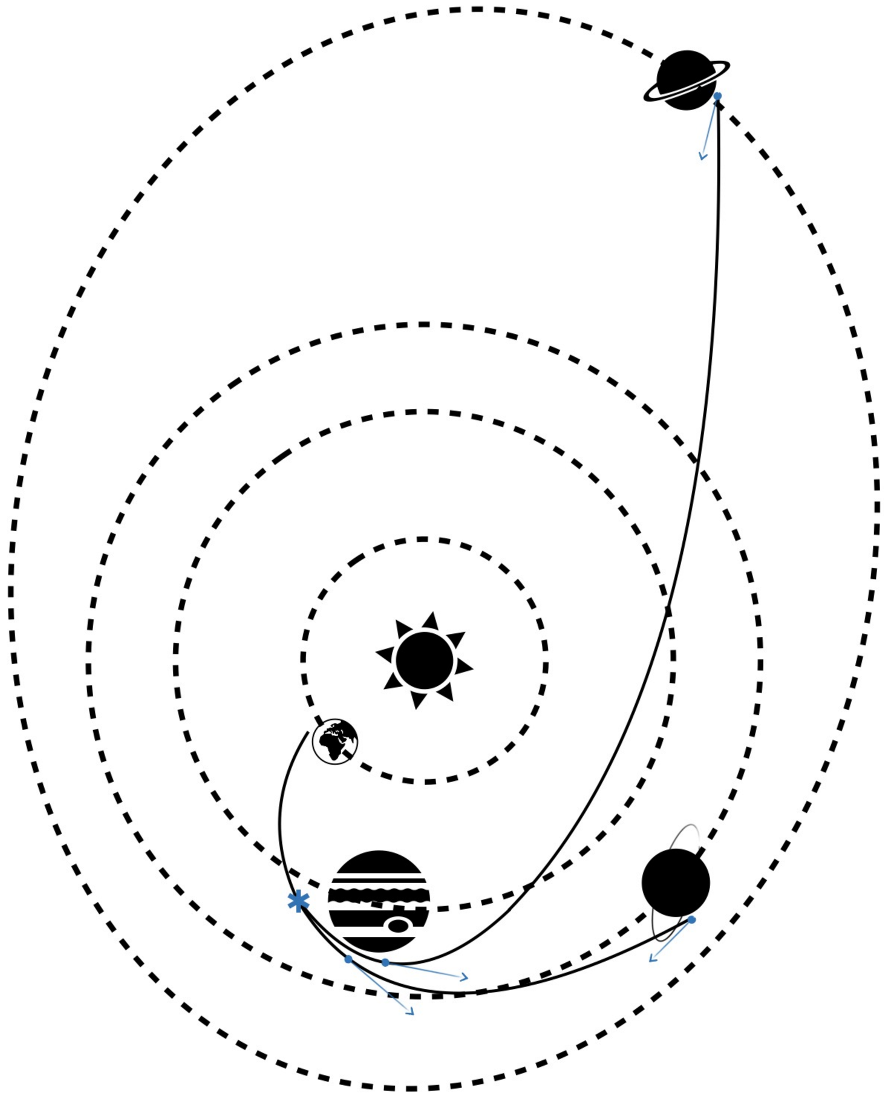

**Figure 3. Diagram to represent the trajectory being modeled. The innermost planet and orbit represent Earth; the next planet is Jupiter; the next planet is Uranus; and the final planet is Neptune. The blue star represents the location where the twin-spacecraft splits into individual spacecrafts. The blue arrows represent thrusting to apply delta-v during powered flybys and orbit insertion maneuvers.**

*Optimization Constraints*. The PMGA optimization problem defined above focuses on finding an optimal trajectory for a single spacecraft traveling to a single destination planet. To expand this analysis to the twin-spacecraft twin-planet mission proposed, the problem execution is modified to incorporate both planets. A trajectory is optimized from Earth to Uranus/Neptune, with the assumption that the spacecraft splits into two spacecrafts before the final Jupiter fly-by. Then, the second trajectory is optimized from Jupiter to Neptune/Uranus. The analysis is repeated with the destinations flipped, as shown below:

1. An optimal trajectory is generated from Earth to Uranus, with planned flybys

2. The spacecraft is assumed to split into two individual spacecrafts immediately before the flyby

3. An optimal trajectory is calculated from flyby planet to Neptune

4. Total $\mathbf{\Delta v}$ for both trajectories, and their sum is calculated

5. Steps 1-4 are repeated with Uranus and Neptune switched, ie, initial optimal trajectory is directed to Neptune, with a branched trajectory to Uranus

This analysis scheme is repeated over a variety of predetermined parameters, such as, different flyby sequences, launch windows, and, orbit capture requirements. It is shown in further detail as follows:

- *Flyby sequences*: Different planetary gravity assists, from the inner solar system planets and the gas giants, are considered. Due to its large gravity well, Jupiter is capable of providing considerable $\mathbf{\Delta v}$, and is included in all sequences considered. Each planet is represented by its first letter in capital: E represents Earth, V represents Venus, M represents Mars, J represents Jupiter, S represents Saturn, U represents Uranus, and N represents Neptune. The sequences considered are EJX, EEJX, EMJX, EEMJX, EMVEX, EMEJX, EVJX, EVEJX, where X represents the final leg of the trajectory, either Neptune, Uranus, or Saturn-Uranus.

- *Launch windows*: Since the analysis is focused on a mission to be designed within the next couple decades, the launch windows considered are 2025 to 2050. Within this window, the optimization is run for every year bound. Missions requiring a Jupiter gravity assist are possible in the 2030s timeframe due to Jupiter's synodic period with Uranus and Neptune. These missions would arrive arrive at the destination planets in the mid 2040s. This launch window allows the spacecrafts to observe the ice giants during Uranus's northern autumnal equinox and Neptune's northern spring equinox—which have never been observed before as Voyager previously only observed the southern hemisphere of Uranus and Neptune.

## RESULTS

This section presents the results for the PMGA optimization problem. The results are displayed as a series of trajectories with the launch and arrival dates, velocity requirements, and planetary gravity assist sequences. Table 1 and Table 2 show the computed results for Uranus-first and Neptune-first optimization respectively. The trajectories listed in Table 1 are designed to be optimized for the Earth-Uranus journey, with a separate optimization run for the Jupiter-Neptune journey. This assumes that the twin-spacecraft launch and travel to Jupiter as a single spacecraft, and split into two spacecrafts before the flyby. The two spacecrafts each have their respective flybys around Jupiter and travel to the ice giants separately. Similarly, the trajectories listed in Table 2 are designed to be optimized for the Earth-Neptune journey, with a separate optimization for the Jupiter-Uranus journey.

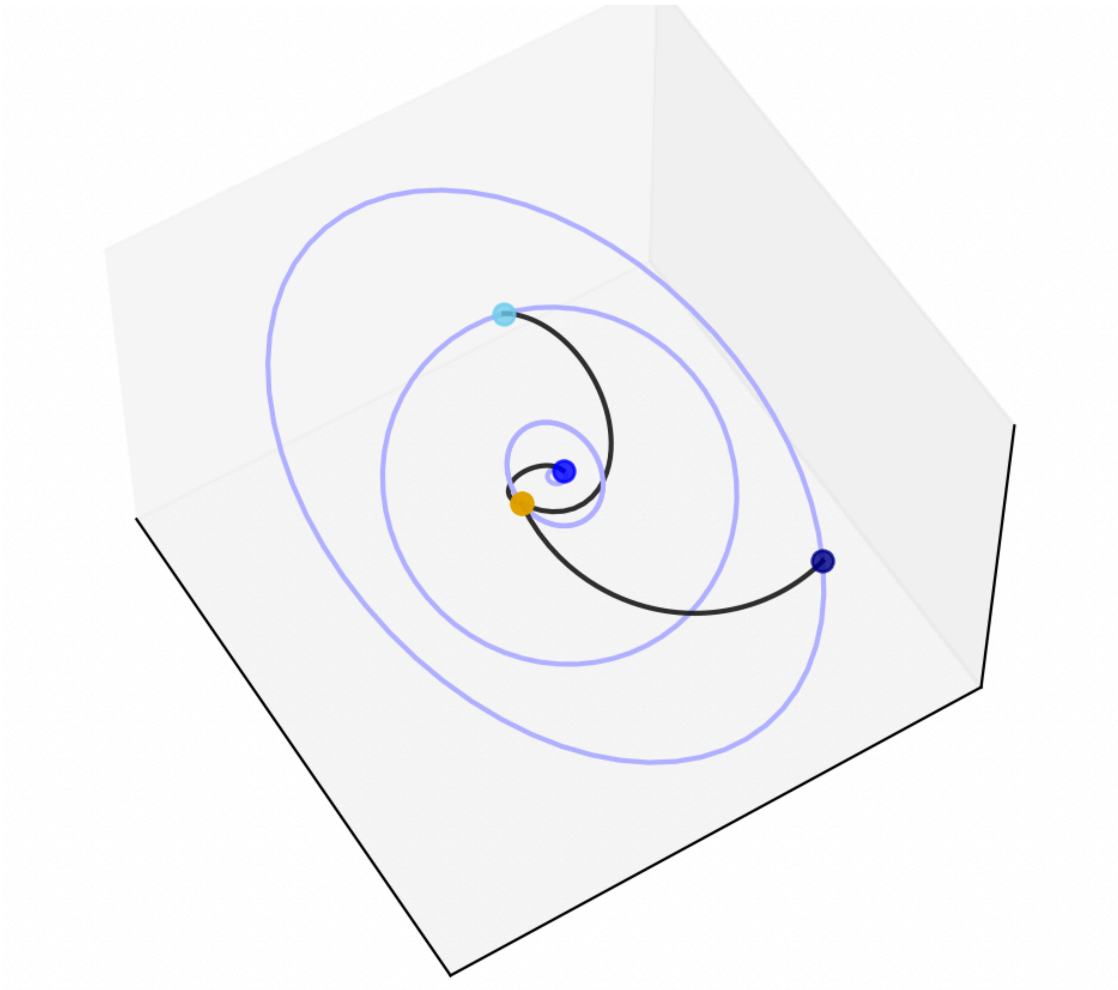

**Figure 5. Trajectory output from the PMGA optimizer. The inner purple marker represents Earth; the middle yellow marker represents Jupiter; the outer blue markers represent Uranus (light blue) and Neptune (dark blue).**

The main parameters to consider in the results are the total $\Delta\mathbf{v}$ and the arrival epochs. The fly-by $\Delta\mathbf{v}$ is calculated by summing all the velocity changes during the powered gravity assist maneuvers,

$$\Delta\mathbf{v}_{flyby} = \sum \Delta\mathbf{v}_{powered\ maneuvers} \tag{15}$$

The arrival $\Delta\mathbf{v}$ is calculated as the sum of the total $\Delta\mathbf{v}_{capture}$ as shown in Equation 7. The total $\Delta\mathbf{v}$ is the sum of all $\Delta\mathbf{v}$s.

**Table 1. Results for the optimized trajectories with Uranus-first optimization scheme. The results are tabulated with increasing $\Delta V$.**

| Launch Epoch | Arrival Epoch - Uranus | Arrival Epoch - Neptune | Sequence | Total $\Delta V$ *km/s* | Flyby $\Delta V$ *km/s* | Arrival $\Delta V$ Uranus *km/s* | Arrival $\Delta V$ Neptune *km/s* |
|---|---|---|---|---|---|---|---|
| 01-10-2030 | 11-29-2051 | 11-30-2051 | EJU<br>EJN | 8.030 | 0.293 | 2.915 | 4.822 |
| 01-02-2029 | 11-21-2050 | 11-22-2050 | EJU<br>EJN | 8.578 | 0.364 | 2.995 | 5.219 |
| 02-20-2042 | 01-10-2064 | 01-11-2064 | EJU<br>EJN | 9.349 | 1.144 | 3.063 | 5.142 |
| 02-09-2041 | 12-30-2062 | 12-31-2062 | EJU<br>EJN | 8.691 | 0.911 | 3.237 | 5.541 |
| 01-02-2028 | 11-21-2049 | 11-22-2049 | EJU<br>EJN | 10.542 | 1.755 | 3.148 | 5.639 |
| 03-07-2043 | 01-24-2065 | 01-25-2065 | EJU<br>EJN | 11.190 | 3.460 | 2.903 | 4.827 |
| 02-01-2040 | 12-21-2061 | 12-22-2061 | EJU<br>EJN | 12.0 | 2.565 | 3.423 | 6.015 |
| 12-15-2026 | 11-03-2048 | 11-04-2048 | EJU<br>EJN | 12.0 | 2.582 | 3.327 | 6.122 |
| 09-07-2026 | 10-07-2046 | 07-29-2048 | EJSU<br>EJN | 12.294 | 2.410 | 3.399 | 6.485 |
| 06-02-2033 | 08-23-2046 | 04-22-2055 | EVJU<br>EVJN | 13.277 | 1.777 | 5.128 | 6.372 |

**Table 2. Results for the optimized trajectories with Neptune-first optimization scheme. The results are tabulated with increasing $\Delta V$.**

| Launch Epoch | Arrival Epoch - Uranus | Arrival Epoch - Neptune | Sequence | Total $\Delta V$ *km/s* | Flyby $\Delta V$ *km/s* | Arrival $\Delta V$ Uranus *km/s* | Arrival $\Delta V$ Neptune *km/s* |
|---|---|---|---|---|---|---|---|
| 01-23-2030 | 12-13-2051 | 12-12-2051 | EJU<br>EJN | 7.75 | 0.013 | 2.930 | 4.805 |
| 02-29-2044 | 11-27-2064 | 01-17-2066 | EJU<br>EJN | 8.17 | 0.712 | 3.045 | 4.417 |
| 11-09-2025 | 09-28-2047 | 09-28-2047 | EEJSU<br>EEJN | 8.7 | 1.157 | 2.631 | 4.914 |
| 03-21-2042 | 01-18-2064 | 02-07-2064 | EJU<br>EJN | 9.57 | 1.304 | 3.205 | 5.064 |
| 02-01-2029 | 12-22-2050 | 12-12-2050 | EJU<br>EJN | 9.67 | 1.528 | 2.926 | 5.216 |
| 02-10-2029 | 08-03-2046 | 12-30-2050 | EEJU<br>EEJN | 9.84 | 0.046 | 4.707 | 5.093 |
| 10-10-2026 | 08-28-2048 | 08-27-2048 | EJSU<br>EJN | 9.86 | 1.295 | 3.346 | 5.223 |
| 03-31-2031 | 11-21-2052 | 02-15-2053 | EJU<br>EJN | 9.88 | 2.655 | 2.787 | 4.443 |
| 09-10-2025 | 07-31-2047 | 03-14-2046 | EJSU<br>EJN | 9.98 | 1.489 | 2.875 | 5.620 |
| 04-09-2043 | 10-06-2063 | 02-25-2065 | EJU<br>EJN | 10 | 2.081 | 3.264 | 4.656 |

Analyzing the results from Table 1, it is observed that the trajectories with a Jupiter gravity assist perform best in terms of the $\mathbf{\Delta v}$ requirements. There are favorable launch opportunities spread throughout the 25 year window; however, most opportunities are in the 2028-2035 period. As stated in the previous section, a launch during this period would be ideal, as it would allow the spacecraft to observe the ice giants in the late 2040s, when both ice giants' northern hemispheres can be studied. Additionally, it is seen that the major contributor to the $\mathbf{\Delta v}$ is due to the high arrival velocity at Neptune, and the subsequent Neptune orbit insertion (NOI) maneuver. This can be addressed by using advanced techniques for orbit insertion, such as aerocapture, which allows to slowly circularize the spacecraft orbit using Neptune's atmospheric drag, and allows for higher $\mathbf{\Delta v}$ reduction. Moreover, Neptune's moon, Triton, could be used for arrival velocity reduction as well—multiple flybys around the moon could be designed to reduce the incident velocity. Doing so would also allow for close observation of Triton, which is already a high priority target for exploration.

Another important observation to draw from the trajectories is how close the arrival dates are at each planet. Approximately half the trajectories arrive at the respective ice giants within a month of each other; this is due to the maximization of the time of flight bound provided in the optimization routine. To reduce the $\Delta\mathbf{v}$ to a minimum, the optimizer creates trajectories with the longest travel time possible. The $\Delta\mathbf{v}$ and time-of-flight relationship is further studied in Figure 5.

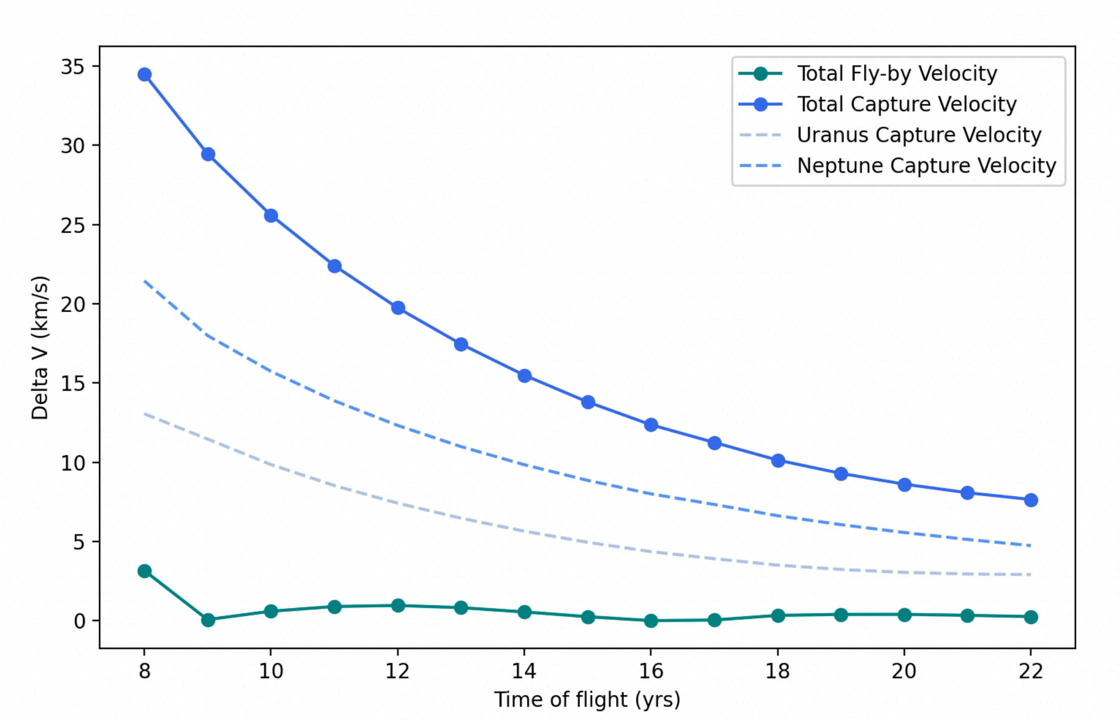


**Figure 5. Variation of flyby and capture $\Delta$v with increasing time-of-flight. The optimization is run for a Neptune-first scheme, for a 2029-2032 launch window, with a Earth-Jupiter-Destination sequence.**

Similarly, analyzing trajectories from Table 2, the trajectories designed with a Neptune-first optimization have multiple optimal gravity-assist sequences that can be implemented. The majority of the sequences are a Jupiter gravity-assist; however, the Earth-Earth-Jupiter-Saturn-Uranus/Earth-Earth-Jupiter-Neptune, the Earth-Jupiter-Saturn-Uranus/Earth-Jupiter-Neptune, and the Earth-Earth-Jupiter-Uranus/Earth-Earth-Jupiter-Neptune sequences provide optimal trajectories with low $\Delta\mathbf{v}$ values as well.

It can be noted that optimizing Neptune-first generates trajectories with a lower overall $\Delta\mathbf{v}$. Neptune being the farther planet has longer flight times and higher arrival velocities compared to Uranus. Thus, identifying the optimal trajectories to minimize $\Delta\mathbf{v}$ for the Earth-Neptune journey and then optimizing the Jupiter-Uranus journey based on the prior produces more optimal results. The Neptune-first optimization scheme also faces similar arrival velocity constraints as described earlier and would benefit from a aerocapture or REP stage to reduce the capture $\Delta\mathbf{v}$ required.

The lowest $\Delta V$ trajectory from Table 2 is analyzed further to observe the relationship between $\Delta\mathbf{v}$ and time-of-flight. Both Table 1 and Table 2 show a group of trajectories launching around the 2030s. To model these, the launch window bounds are reduced to 2029-2032. To generalize the analysis over the gravity-assist sequences, only an Earth-Jupiter-Neptune and Earth-Jupiter-Uranus sequence is modeled. The time-of-flight is varied from 8 to 22 years, and the corresponding flyby and capture $\Delta\mathbf{v}$s are calculated for both ice giants. The analysis is repeated for a Uranus-first optimization scheme, and shows the same results. As seen in Figure 5, the capture velocity required exponentially increases with a decrease in travel time. While it is unreasonable to fly missions with <10 year travel times because of the high $\Delta\mathbf{v}$, it is also impractical to have a mission flight-time of >15 years.

For missions in the 12-16 year time-of-flight range, it is imperative for the spacecraft to have novel propulsion techniques to support successful capture. Additionally, the high velocity capture at Neptune can be avoided by modifying the mission architecture to fly by Neptune and send a probe to the surface, instead of orbiting around Neptune. This architecture could be modified to incorporate a tour of Triton and other Kuiper belt objects.

## CONCLUSION

This research identifies feasible and optimal trajectories for a twin-spacecraft single-launch mission to the ice giants. Trajectories with a possible launch between 2025-2050 are considered. Multiple planetary flyby sequences are implemented and evaluated. The results show that there exist trajectories for the dual mission proposed. There is a window of conducive launch opportunities in the 2029-2033 time period, which with a time-of-flight of 12-15 years will bring the spacecrafts to the ice giants during the coveted period of the planets' northern equinox.

Further analysis shows that to successfully implement a twin-planet mission that satisfies both the $\Delta\mathbf{v}$ and time-of-flight constraint, the mission architecture must be modified to include novel options (REP, aerocapture, SEP) or be modified to an orbiter at Uranus and a flyby about Neptune.

Future work could include modeling solar electric propulsion (SEP) for the first half of the trajectory. This could significantly affect the payload mass and the arrival velocities at the ice giants.


## ACKNOWLEDGMENTS

I would like to express my deepest gratitude to my advisor Dr. Brian Gunter. His mentorship, guidance, and encouragement was invaluable to the success of this project and my growth as an engineer.

This research work would not have been possible without the support and motivation from my family and friends. Mom, Dad, Shawn, Ankita, Rikhi, and Comet, I am forever grateful.


## REFERENCES


[1] *Bate, Roger R., et al. Fundamentals of Astrodynamics. Dover Publications INC, 2020.*

[2] Fletcher, L. N., et al. "Ice Giant System Exploration in the 2020s: an Introduction." *Philosophical Transactions of the Royal Society A: Mathematical, Physical and Engineering Sciences*, vol. 378, no. 2187, 2020, p. 20190473., doi:10.1098/rsta.2019.0473.

[3] Guo, Yanping, and Robert W. Farquhar. "New Horizons Mission Design." *New Horizons*, pp. 49–74., doi:10.1007/978-0-387-89518-5_4.

[4] Hofstadter, Mark D., et al. “Future Missions to the Giant Planets That Can Advance Atmospheric Science Objectives.” *Space Science Reviews*, vol. 216, no. 5, 2020, doi:10.1007/s11214-020-00710-w.

[5] Hofstadter, Mark, et al. “Uranus and Neptune Missions: A Study in Advance of the next Planetary Science Decadal Survey.” *Planetary and Space Science*, vol. 177, 2019, p. 104680., doi:10.1016/j.pss.2019.06.004.

[6] Huaura Solórzano, Carlos Renato, et al. “Analysis of Trajectories to Neptune Using Gravity Assists.” *The Journal of the Astronautical Sciences*, vol. 54, no. 3-4, 2006, pp. 583–593., doi:10.1007/bf03256507.

[7] Izzo, D., et al. “Search Space Pruning and Global Optimisation of Multiple Gravity Assist Spacecraft Trajectories.” *Journal of Global Optimization*, vol. 38, no. 2, 2006, pp. 283–296., doi:10.1007/s10898-006-9106-0.

[8] Izzo, Dario. “Global Optimization and Space Pruning for Spacecraft Trajectory Design.” *Spacecraft Trajectory Optimization*, pp. 178–201., doi:10.1017/cbo9780511778025.008.

[9] Kim Reh. “Solar System Planetary Science Decadal Survey and Missions in the next Decade, 2013–2022.” *2011 Aerospace Conference*, 2011, doi:10.1109/aero.2011.5747292.

[10] Mansell, J., et al. “Oceanus: A Multi-Spacecraft Flagship Mission Concept to Explore Saturn and Uranus.” *Advances in Space Research*, vol. 59, no. 9, 2017, pp. 2407–2433., doi:10.1016/j.asr.2017.02.012.

[11] Masters, A., et al. “Neptune and Triton: Essential Pieces of the Solar System Puzzle.” *Planetary and Space Science*, vol. 104, 2014, pp. 108–121., doi:10.1016/j.pss.2014.05.008.

[12] Mereta, Alessio, and Dario Izzo. “Target Selection for a Small Low-Thrust Mission to near-Earth Asteroids.” *Astrodynamics*, vol. 2, no. 3, 2018, pp. 249–263., doi:10.1007/s42064-018-0024-y.

[13] Olds, Aaron D., et al. “Interplanetary Mission Design Using Differential Evolution.” *Journal of Spacecraft and Rockets*, vol. 44, no. 5, 2007, pp. 1060–1070., doi:10.2514/1.27242.

[14] Prussing, John E., and Bruce A. Conway. *Orbital Mechanics*. Oxford University Press, 2013.

[15] “Pykep.” *PyPI*, pypi.org/project/pykep/.

[16] Russell, Ryan P. “Survey of Spacecraft Trajectory Design in Strongly Perturbed Environments.” *Journal of Guidance, Control, and Dynamics*, vol. 35, no. 3, 2012, pp. 705–720., doi:10.2514/1.56813.

[17] Simon, Amy A., et al. “Outer Solar System Exploration: A Compelling and Unified Dual Mission Decadal Strategy for Exploring Uranus, Neptune, Triton, Dwarf Planets, and Small KBOs and Centaurs.” *ArXiv.org*, 30 Aug. 2019, arxiv.org/abs/1807.08769.

[18] Spilker, Thomas R., et al. “Qualitative Assessment of Aerocapture and Applications to Future Missions.” *Journal of Spacecraft and Rockets*, vol. 56, no. 2, 2019, pp. 536–545., doi:10.2514/1.a34056.

[19] Turrini, Diego, et al. “The Comparative Exploration of the Ice Giant Planets with Twin Spacecraft: Unveiling the History of Our Solar System.” *Planetary and Space Science*, vol. 104, 2014, pp. 93–107., doi:10.1016/j.pss.2014.09.005.

[20] Vasile, M., and P. De Pascale. “Preliminary Design of Multiple Gravity-Assist Trajectories.” *Journal of Spacecraft and Rockets*, vol. 43, no. 4, 2006, pp. 794–805., doi:10.2514/1.17413.

[21] Vasile, M., et al. “Analysis of Some Global Optimization Algorithms for Space Trajectory Design.” *Journal of Spacecraft and Rockets*, vol. 47, no. 2, 2010, pp. 334–344., doi:10.2514/1.45742.

[22] Zangari, Amanda M., et al. “Return to the Kuiper Belt: Launch Opportunities from 2025 to 2040.” *Journal of Spacecraft and Rockets*, vol. 56, no. 3, 2019, pp. 919–930., doi:10.2514/1.a34329.